

Double J-shaped Kirschner wire fixation provides superior biomechanical stability for feline sacroiliac luxation compared with conventional techniques

Sang-Kun Jang, DVM ; Yookyeong Lee, DVM ; Sangyul Lee, DVM ; Jaewon Do, DVM ; Jeong-Woon Kim, DVM, MS ; Jun-Sik Cho, DVM, MS ; Hwi-yool Kim, DVM, PhD ; Jung-Moon Kim, DVM, PhD* 

Department of Veterinary Surgery, College of Veterinary Medicine, Konkuk University, Seoul, Republic of Korea

*Corresponding author: Dr. Kim (kimjungm418@gmail.com)

Objective

To compare the biomechanical stability of 3 fixation techniques for unilateral sacroiliac (SI) luxation using 3-D-printed feline pelvic models.

Methods

Eighteen 3-D-printed pelvic models were generated from CT data of a 6.6-kg cat. The study was conducted from July 25 through September 10, 2025. A right SI luxation with ipsilateral pubic and ischial osteotomies was created, and models were fabricated for 3 fixation configurations (n = 6/group): single lag screw with transiliac pinning (SP), double parallel Kirschner wires (DK), and double J-shaped Kirschner wires (DJ). A 3-D-printed femur was toggle pinned to the acetabulum to reproduce stance. Axial compression was applied to the femoral head at 5 mm/min to 15° pelvic rotation. Outcomes included rotational stiffness (primary), maximum load at 10° rotation, and energy absorption.

Results

DJ constructs showed approximately 3-fold greater initial rotational stiffness and higher energy absorption than SP and DK. Mean maximum load to 10° rotation was 93.10 N for DJ versus 33.32 N (SP) and 36.59 N (DK). No differences were detected between SP and DK for any parameter.

Conclusions

In this ex vivo 3-D-printed model, DJ fixation provided superior rotational stability compared with SP and DK techniques.

Clinical Relevance

The DJ technique may offer a biomechanically robust alternative for stabilizing feline SI luxation. By avoiding the narrow sacral safe corridor required for lag screw placement, this method may reduce the risk of iatrogenic nerve injury while preserving sacral bone integrity to ensure optimal purchase and minimize the risk of fixation failure during stabilization.

Keywords: sacroiliac luxation, feline biomechanics, J-shaped K-wire fixation, rotational stability, 3-D-printed pelvic model

Sacroiliac (SI) joint luxation is the second most common traumatic pelvic injury in cats and frequently requires surgical stabilization.^{1,2} Approximately 15% of feline cases are bilateral.^{1,3} While conservative management may be appropriate when iliac displacement from the sacrum is minimal,⁴ surgical stabilization is indicated in patients with severe pain, neurologic deficits, or pelvic canal stenosis or when

rapid return to weight-bearing is desired.³ In bilateral cases, surgical fixation can alleviate discomfort, hasten recovery, and help maintain the physiologic width of the pelvic canal.²

The current standard surgical technique for SI stabilization is lag screw fixation, inserting a screw from the ilium into the sacral body.⁵ To optimize purchase, guidelines recommend maximizing screw diameter and achieving a screw span of at least 60% of the sacral body width while maintaining an intraosseous path.^{6,7} However, feline sacral anatomy presents considerable challenges: the safe insertion area is extremely small (approx 0.5 cm², approx 25%

Received November 28, 2025

Accepted January 27, 2026

Published online February 17, 2026

doi.org/10.2460/ajvr.25.11.0422

© 2026 THE AUTHORS. Published by the American Veterinary Medical Association as an Open Access article under Creative Commons CCBY-NC license.

of the articular surface of the sacral wing) and is surrounded by critical structures, such as the spinal canal, nerve roots, lumbosacral disk space, and pelvic canal.⁸ In addition, individual variation of sacral shape and articular surface angles can complicate achieving an ideal intraosseous trajectory on the first attempt. Repeated drilling may compromise bony purchase,^{8,9} and the use of small-diameter Kirschner (K) wires for pilot holes has been suggested to reduce malpositioning.⁸

Recent biomechanical investigations have emphasized rotational and torsional loading as the common failure modes in SI joint fixation constructs. Two-point fixation across the joint has been shown to increase construct stiffness, yield load, and peak load compared with single long lag screws in canine models.^{10,11} Similarly, fixation using 2 smaller headless compression screws demonstrated greater resistance to rotational forces than a single larger cortical screw placed in lag fashion.¹² Parallel results have been reported for pin-based constructs, where transiliac pinning, double K-wire fixation, and tricortical configurations provide enhanced stability through multipoint, spatially distributed fixation.¹³⁻¹⁵

These findings collectively suggest that the number and spatial distribution (span) of fixation points may be as crucial as implant size in resisting rotational forces at the SI joint. Nevertheless, there is a lack of biomechanical evidence directly comparing such spatially distributed, multipoint fixation strategies in feline SI stabilization. Based on this rationale, this study hypothesized that a newly developed double J-shaped K-wire configuration (DJ) intended to simplify application and reduce reinsertion-related complications through spatially distributed multipoint fixation would provide greater rotational stability than 2 established methods: a single lag screw with transiliac pinning (SP) or a parallel double K-wire configuration (DK). Thus, this study aimed to biomechanically compare the rotational stability of the DJ technique versus these 2 established methods using 3-D-printed feline pelvic models under physiologic alignment.

Methods

3-D model design and fabrication—Eighteen pelvic and right femur models ($n = 6/\text{group}$) were developed based on a CT scan of a 5-year-old 6.6-kg intact male Korean shorthair cat with no skeletal abnormalities. The CT data were processed and converted into .stl files by CustoMedi. A unilateral (right) SI luxation was digitally simulated using 3-D-modeling software (3D Slicer, version 5.8.1; slicer.org)¹⁶ by detaching the right sacrum from the ilium. To ensure consistent positioning on the universal testing machine jig, square bases were integrated into the models. A base on the pelvic model was aligned parallel to the sacral spinous process, and a base on the distal femur was designed (**Figure 1**) to maintain a 114° hip joint angle and 6° abduction angle during testing (**Figure 2**).^{17,18} All models were fabricated using a fused deposition modeling printer with polycarbonate (PC) material (natural color).¹⁹ Key print

settings were a layer height of 0.18 mm, a wall thickness of 3.6 mm (to mimic the cortex), and a 60% hexagonal infill with an infill line width (mesh thickness) of 0.4 mm (to mimic the medullary mesh).

Surgical implants

The implants used for stabilization were 1.2-mm K-wires (Top Medical Co) and 2.0-mm \varnothing , 24-mm-length, self-tapping titanium cortical screws (Jeil Medical).

Surgical procedures (experimental groups)

All implant trajectories were preplanned during the 3-D-modeling phase, and pilot holes were performed during the 3-D-printing process to ensure consistent placement.

Group 1: SP—A 1.2-mm K-wire was inserted for transiliac pinning, guided by a preformed 1.2-mm pilot hole. For the single lag screw, a preformed 1.2-mm pilot hole was used as a guide. A 2.0-mm glide hole was created in the ciscortex (ilium) using a 2.0-mm drill bit, and a 1.5-mm thread hole was drilled in the transcortex (sacrum) using a 1.5-mm drill bit. A 2.0-mm cortical screw (24-mm length) was then inserted in lag fashion, achieving a screw span of 69% of the sacral width.^{6,7} Screw tightening was performed manually to achieve initial fixation snugness (finger-tight resistance; **Figure 3**).

Group 2: DK—Two 1.2-mm K-wires were used. The pin positions were preplanned during 3-D modeling and accurately placed, guided by 0.9-mm pilot holes that were preformed in the model. The 2 pins were placed parallel to each other within the safe surgical corridor. The external tips of the K-wires were bent near the iliac cortex to prevent potential soft tissue irritation and implant loosening (**Figure 3**).¹⁴

Group 3: DJ—Two 1.2-mm K-wires were used. The entry points and all implant dimensions (long portion, short portion, and transverse portion) were preplanned during the 3-D-modeling phase based on the specific model anatomy to ensure safety and maximize fixation stability. The 2 “long-portion entry points” were located within the established safe surgical corridor, identical to the pin positions in group 2. The “short-portion entry points” were selected to maximize the distance from the long-portion entry points while maintaining anatomical safety, specifically ensuring a minimum distance of 3 mm from the spinal canal based on model-based measurements performed prior to testing.¹⁰ The preplanned dimensions were as follows: pin 1 (38-mm long portion, 8.1-mm short portion, and 2.5-mm transverse portion) and pin 2 (38-mm long portion, 10.6-mm short portion, and 3.3-mm transverse portion; **Figure 4**).

The J shape was created using an in situ bending technique, performed in the following steps:

1. First, a straight 1.2-mm K-wire was inserted into the “long-portion entry point,” guided by a preformed pilot hole.
2. The wire was advanced until a sufficient length, greater than the preplanned “short-portion” length, remained outside the entry point.

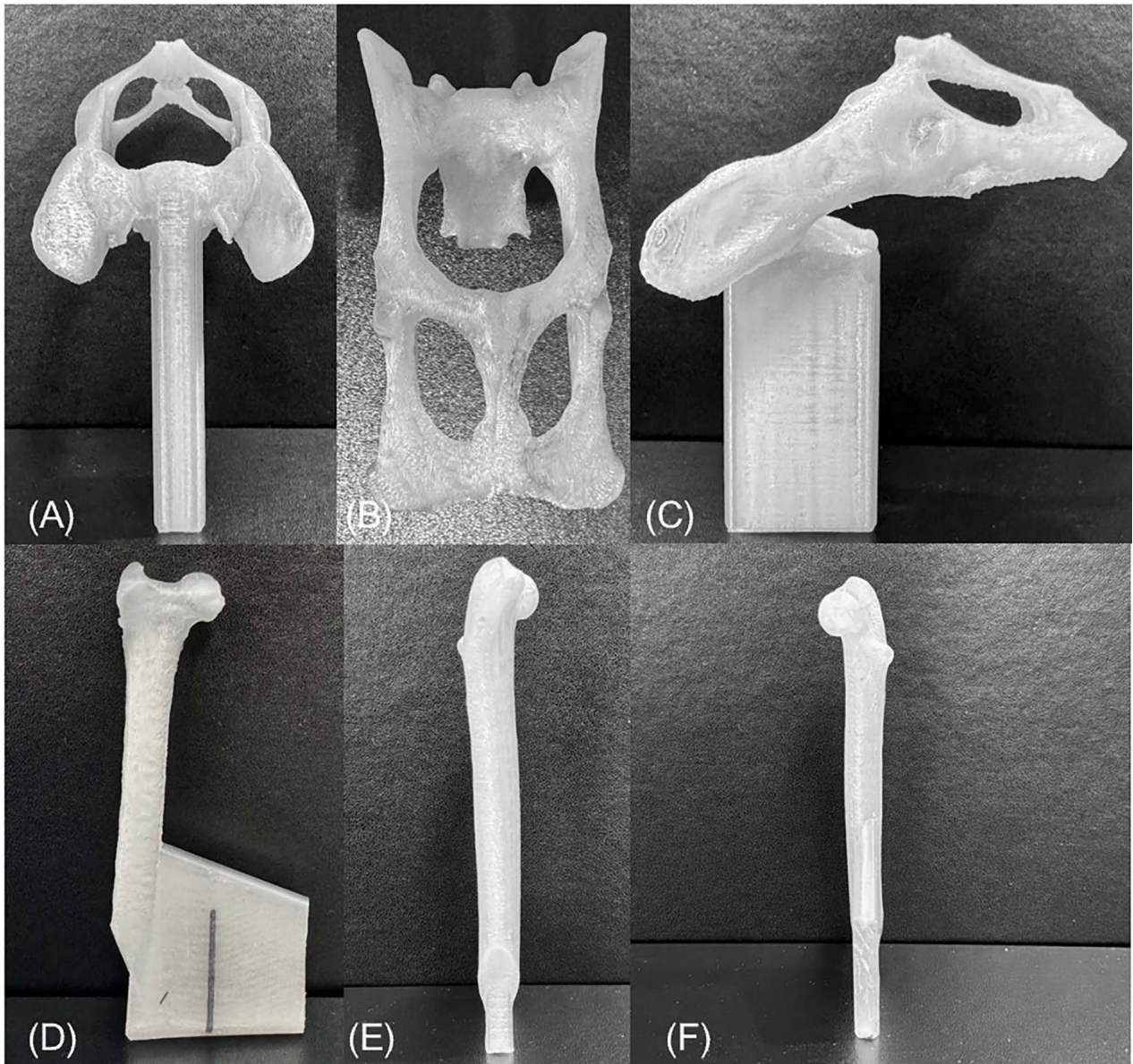


Figure 1—Photographs of the 3-D-printed feline pelvic and right femoral models used to evaluate sacroiliac (SI) stabilization techniques (study period: July through September 2025). The models were fabricated with square bases to facilitate standardized biomechanical testing. The pelvic model is shown in cranial (A), ventral (B), and lateral (C) views; the right femoral model is shown in cranial (D), lateral (E), and medial (F) views. These models served as the anatomical basis for the 3 fixation constructs (single trans-SI lag screw with transiliac pinning [SP], double parallel Kirschner [K] wire transiliosacral pinning [DK], and double J-shaped K-wire transiliosacral pinning [DJ]) evaluated in this study.

3. The external portion of the K-wire was then bent in situ to create the J shape according to the pre-planned transverse and short portion dimensions.
4. Finally, the newly formed short portion was impacted into the “short-portion entry point” using a mallet (Figure 3).

Biomechanical test

All constructs (n = 6/group) were tested using a universal testing machine (Minos-100S; MTDI). To connect the femur model to the pelvic model, toggle pinning was performed using number 2 braided composite suture (FiberWire; Arthrex). The pubis

and ischium were subsequently cut using an oscillating saw to isolate the SI joint’s contribution to stability and prevent any potential interference from the pelvic symphysis during testing.¹⁰ All samples were stabilized at the hip joint through this toggle pinning technique to ensure consistent positioning during testing (Figure 2). The hip joint was fixed at 114° of flexion-extension and 6° of abduction to simulate a mid-to-late stance posture in cats and optimize load axis alignment through the SI joint.

This angle represents an intermediate value between the mean stance angle (approx equal to 104°) reported by Guillot et al¹⁷ and the maximum

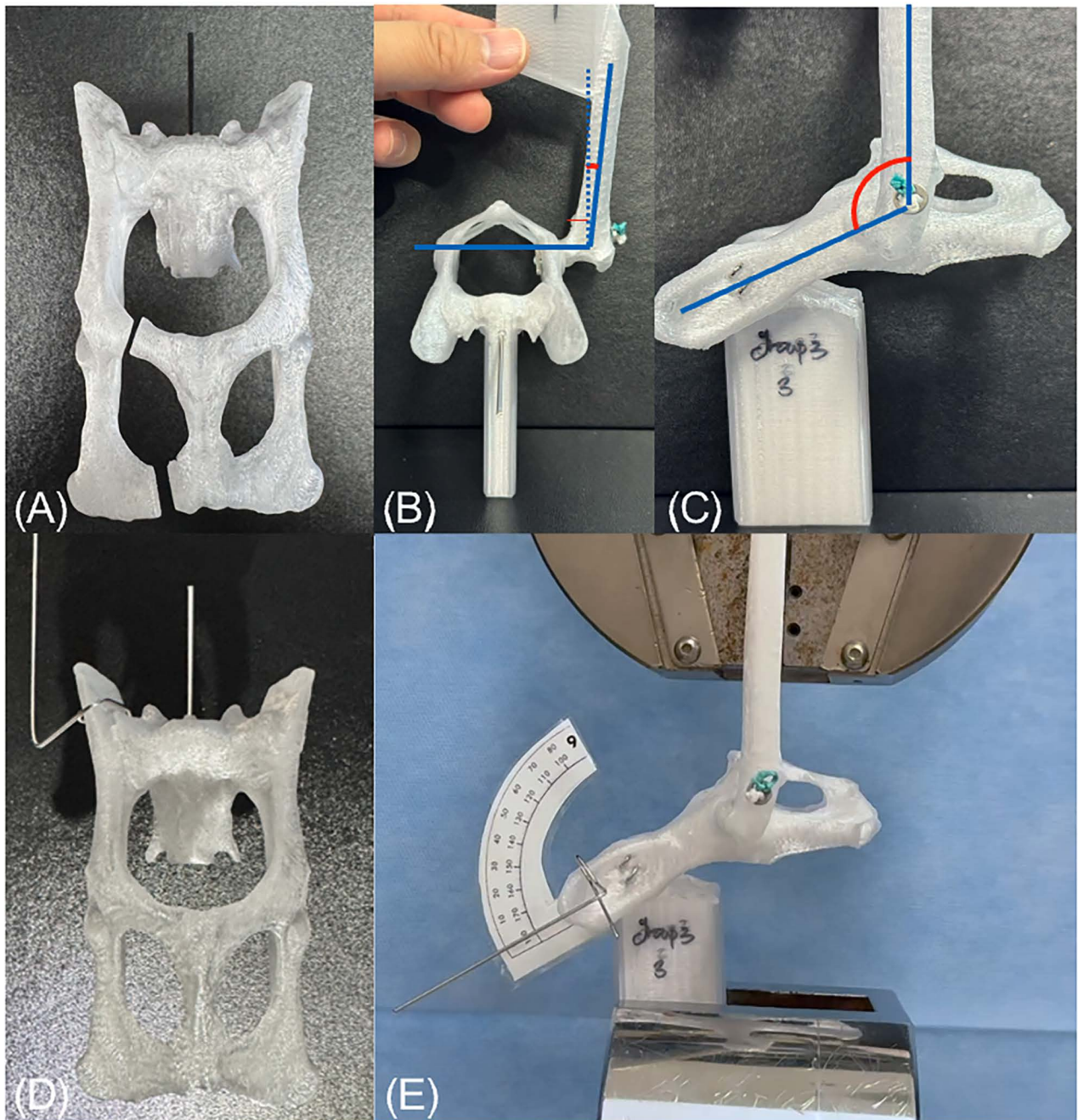


Figure 2—Biomechanical testing setup and 3-D model configuration. The figure illustrates the configuration of the 3-D-printed pelvic model and the biomechanical testing setup. A—The pelvic model with pubic and ischial osteotomies. The femur model was positioned to maintain a 6° abduction angle (B) and a 114° hip joint (flexion-extension) angle (C). D—A close-up view of the goniometer, with the anchor and pointer aligned parallel to each other and to the axis of the sacral spinous process for accurate angle measurement. E—The assembled construct, demonstrating pelvis-femur connection via toggle pinning, the fixed angular position during testing, and measurement of rotational displacement with the goniometer.

extension (approx equal to 130°) described by Brown et al.¹⁸ A vertical compression force test was conducted at a speed of 5 mm/min until ultimate failure. To accurately measure rotational displacement, a goniometer was attached to an anchor installed on the square base of the pelvic model. This anchor was oriented parallel to the sacral spinous process (sagittally), aligning the goniometer's reference with the

axis parallel to the direction of the vertical jig compression (Figure 2). During the test, load (Newtons) and displacement (millimeters) data were continuously recorded. Load values at specific rotational angles (2°, 5°, 10°, and 15°) were extracted for analysis. The primary failure load for comparison was defined as the load required to cause 10° of rotation (corresponding to 4.9 mm of vertical displacement).¹⁰

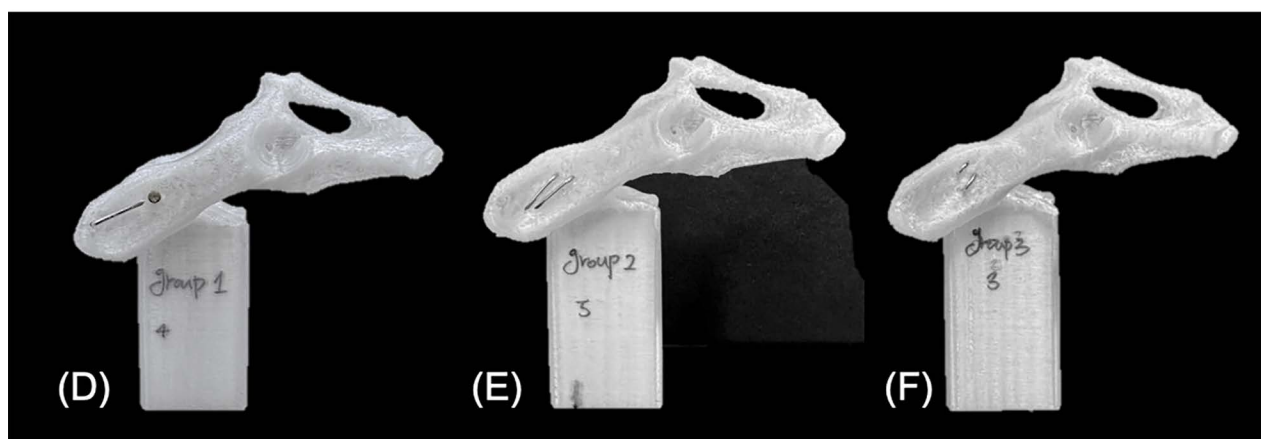
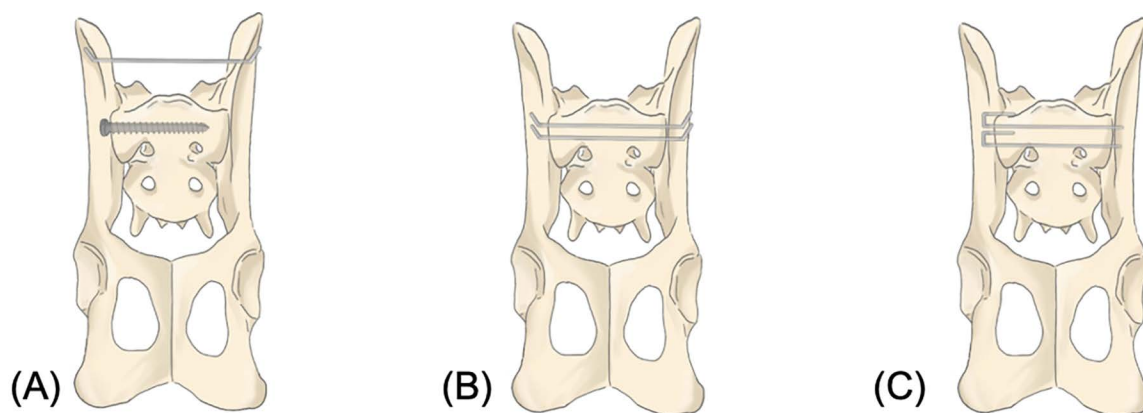


Figure 3—Illustrations and 3-D-printed models demonstrating 3 fixation methods for unilateral SI joint stabilization in feline pelvic models. Ventral-view illustrations show the SP technique (A), the DK technique (B), and the DJ technique (C). Lateral-view 3-D-printed constructs correspond to the SP (D), DK (E), and DJ (F) configurations.

Stiffness for each interval was calculated as the average slope (secant stiffness) between the rotational end points. Work to failure was measured up to 10° rotation and calculated as the area under the load-displacement curve to this displacement.

Statistical analysis

All statistical analyses were performed using statistical software (SPSS Statistics, version 31.0; IBM Corp). Due to the small sample size in each group ($n = 6$), a normal distribution of data could not be assumed; therefore, nonparametric tests were selected.

The Kruskal-Wallis 1-way ANOVA was used to compare differences among the 3 groups. When a significant overall difference was detected, pairwise Mann-Whitney U tests with Bonferroni correction were subsequently performed for multiple comparisons. The reported P values are Bonferroni adjusted. Statistical significance was accepted at $P < .05$ for the Kruskal-Wallis test and at adjusted $P < .05$ (α adjusted = .0167) for post hoc comparisons.

Results

A total of eighteen 3-D-printed feline pelvic models were prepared, with 6 models fabricated for each fixation configuration (SP, DK, and DJ). During

axial compression testing, the DJ constructs showed greater rotational stiffness than the SP and DK constructs, particularly in early rotation (**Table 1**). Mean \pm SD stiffness at 0° to 2° rotation was greater for DJ (24.25 ± 8.46 N/degree) than in SP (7.92 ± 5.22 N/degree; adjusted $P = .018$) and DK (7.59 ± 4.73 N/degree; adjusted $P = .015$), whereas SP and DK did not differ (adjusted $P = .99$). At 2° to 5° rotation, mean stiffness of DJ (9.15 ± 2.73 N/degree) exceeded SP (2.37 ± 1.00 N/degree; adjusted $P = .006$) and DK (2.78 ± 1.06 N/degree; adjusted $P = .009$), with no difference between SP and DK (adjusted $P = .99$). At 5° to 10° rotation, stiffness of DJ (10.04 ± 3.14 N/degree) was greater than in SP (3.27 ± 1.01 N/degree; adjusted $P = .006$), whereas other group comparisons were not significant.

Maximum load resistance and energy absorption followed a similar pattern (Table 1). Maximum load to 10° rotation was significantly greater for DJ (93.10 ± 14.26 N) than for SP (33.32 ± 10.59 N; adjusted $P = .018$) and DK (36.59 ± 11.24 N; adjusted $P = .018$), whereas SP and DK showed no difference (adjusted $P = .657$). Similarly, at 15° rotation, DJ maximum load (107.15 ± 17.12 N) exceeded SP (36.10 ± 9.20 N; adjusted $P = .009$) and DK (44.43 ± 11.46 N; adjusted $P = .006$). Energy absorbed to 10° rotation

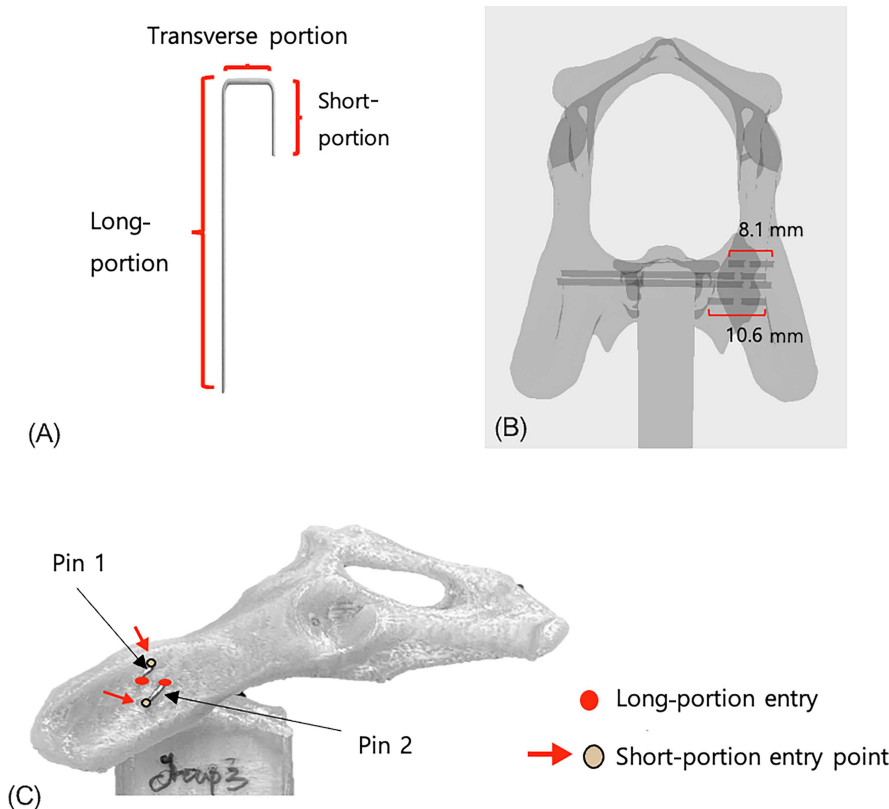


Figure 4—The preoperative planning and placement of J-shaped K-wires for the DJ fixation. A—Schematic illustration of the J-shaped K-wire used in this group, indicating its long, transverse, and short portions. B—Preoperative planning on the 3-D pelvic model, including measurement of the short portions (8.1 and 10.6 mm) and determination of the long and transverse trajectories. C—Final placement of 2 J-shaped K-wires in the 3-D-printed pelvic model in lateral view, where the long-portion entry points are marked with red dots and the short-portion entry points with red arrows and yellow dots.

Table 1—Biomechanical outcomes (rotational stiffness, maximum load, and energy absorption) for 3 fixation constructs in a 3-D-printed feline sacroiliac (SI) luxation model.

Outcome (unit)	SP (n = 6)	DK (n = 6)	DJ (n = 6)
Rotational stiffness, 0–2° (N/degree)	7.92 ± 5.22 (2.45–14.21) ^a	7.59 ± 4.73 (2.45–15.68) ^a	24.25 ± 8.46 (13.23–38.22) ^b
Rotational stiffness, 2–5° (N/degree)	2.37 ± 1.00 (0.49–3.43) ^a	2.78 ± 1.06 (1.47–3.92) ^a	9.15 ± 2.73 (4.90–12.74) ^b
Rotational stiffness, 5–10° (N/degree)	3.27 ± 1.01 (1.96–4.90) ^a	5.72 ± 2.90 (3.43–11.27) ^{a,b}	10.04 ± 3.14 (6.86–15.19) ^b
Maximum load to 10° (N)	33.32 ± 10.59 (20.58–46.06) ^a	36.59 ± 11.24 (23.52–53.90) ^a	93.10 ± 14.26 (71.54–115.64) ^b
Maximum load to 15° (N)	36.10 ± 9.20 (24.50–48.02) ^a	44.43 ± 11.46 (30.38–63.70) ^a	107.15 ± 17.12 (79.38–129.36) ^b
Energy absorbed to 10° (mJ)	146.46 ± 61.13 (64.29–245.77) ^a	137.71 ± 59.54 (75.61–227.83) ^a	433.65 ± 96.58 (326.14–580.10) ^b

Values are mean ± SD (range). Adjusted *P* values of 1.000 are reported as *P* < .99 in accordance with AVMA journal style. A total of eighteen 3-D-printed feline pelvic models (n = 6/group) were tested from August through September 2025 to compare the rotational stability of 3 techniques: single 2.0-mm lag screw and 1.2-mm transiliac pinning (SP), 2 parallel 1.2-mm K-wires (DK), and two 1.2-mm double J-shaped K-wires (DJ).

K = Kirschner.

^{a,b}Significant differences (*P* < .05) based on Bonferroni-adjusted post hoc tests.

for DJ (433.65 ± 96.58 mJ) was notably higher than for SP (146.46 ± 61.13 mJ; adjusted *P* = .006) and DK (137.71 ± 59.54 mJ; adjusted *P* = .007), with no difference between SP and DK (adjusted *P* = .99).

Discussion

To the authors' knowledge, this is the first study to demonstrate that a DJ technique provides superior rotational stiffness and energy absorption in a feline SI luxation model, supporting its potential as a clinically

advantageous alternative to established methods. Consistent with this, the DJ technique provided markedly greater rotational stability than both the conventional SP technique and the DK technique. The DJ technique demonstrated statistically superior performance across all measured parameters, including initial stiffness, stiffness during later rotation intervals, maximum load to 10° and 15° rotation, and work to failure (Table 1). This indicates that the DJ construct provides greater resistance from initial micromotion up to and beyond the defined clinical failure point (10° rotation).

Standardized criteria for defining biomechanical failure of SI joint fixation remain lacking. In this study, clinical failure was defined as 10° of rotational displacement. This definition was based on translation of the 5-mm vertical displacement criterion used by Hanlon et al¹⁰ in canine SI joint evaluation to the rotational equivalent in our model geometry (approx 4.9-mm vertical displacement corresponded to 10° rotation). Although standardized criteria for biomechanical failure in SI joint fixation are lacking, the criterion used in this study was adopted for comparability with this previous key study.¹⁰

Notably, the work-to-failure (approx 434 mJ) for the DJ group was nearly 3 times higher than that of the other 2 groups (approx 146 and 138 mJ, respectively), suggesting a much tougher construct capable of absorbing significantly more energy before failure (Table 1). This high energy absorption capacity may translate to better resistance against impact forces experienced during activities like jumping or falling.²⁰ Indeed, the mean maximum load sustained by the DJ constructs (93 N at 10° and 107 N at 15°) exceeded the reported average peak vertical ground reaction force during landing from a 1-m height in cats (approx 91 N).²⁰ In contrast, the maximum loads for groups 1 and 2 were only comparable to or slightly above the forces generated during walking (PVF approx equal to 40% to 50% body weight) or trotting (PVF approx equal to 50% to 60% body weight).²¹ This suggests that the DJ technique potentially offers greater stability margin for maintaining SI joint reduction even during high-impact activities.

Interestingly, no significant differences were found between SP (group 1) and the DK (group 2) for any measured parameter. This suggests that simply using 2 parallel K-wires may not offer superior rotational stability compared to a single screw (plus pin) fixation. Accordingly, the superior performance of DJ likely reflects differences in fixation geometry and point distribution rather than fixation number alone.

The superior performance of the DJ technique (group 3) can be attributed to its unique multi-point fixation strategy and the intrinsic properties of K-wires. Unlike the parallel pins in group 2, the DJ technique creates 4 spatially distributed fixation points via the long and short portions of each J-pin. The short portion provides additional purchase in the ilium and parts of the sacrum, potentially acting similarly to the principle of increased stability from tricortical support reported for K-wire fixation in previous contexts.¹⁵ This spatial arrangement appears critical for enhancing rotational stability. According to structural mechanics principles, the distance between fixation points (span) significantly influences rotational resistance. While increasing span initially increases the resisting moment arm ($M_r = F \times s$) (M_r = resisting moment, F = fixation point, s = excessive span), excessive span can lead to increased bending deformation, reducing overall torsional stiffness, suggesting that an optimal span exists for maximum stability.^{22,23} The closely spaced parallel pins in group 2 may have had a suboptimal span. Conversely, the DJ technique, by distributing

fixation points via the long and short portions, likely achieved an arrangement closer to a biomechanically advantageous optimal span, thereby maximizing rotational resistance.

These observations also contrast with the results of Hanlon et al,¹⁷ who reported that 2 short positional screws provided significantly greater stiffness, yield load, and peak load compared to a single long lag screw in canine SI joint fixation. Several factors might explain this discrepancy. First, the double screws in the Hanlon et al¹⁷ study likely achieved rigid initial fixation within the bone, contributing significantly to stability through their defined span. Conversely, the 2 K-wires in our group 2 were placed relatively close together, and K-wires generally offer poorer purchase in bone compared to screws. This configuration might not have provided a sufficient structural advantage to effectively resist rotational moments. This highlights that not only the “number” but also the “quality of fixation” and the “spatial arrangement” of fixation points are critical to achieving rotational stability.

The short-portion entry points were meticulously preplanned to maximize distance from the long-portion points while ensuring safety relative to anatomical structures, like the spinal canal. Considering the narrow safe corridors in the feline sacrum and ilium,^{8,9,24,25} such 3-D model-based preplanning remains crucial for clinical application. In this phase, the thickest possible K-wire is selected, and its short portion's length is predetermined. Since the J shape is prebent before insertion, the depth is inherently controlled by the implant's geometry. Furthermore, even if the short portion deviates from the intended corridor, its trajectory inherently directs the tip away from the pelvic canal, enhancing the safety margin. Clinically, creating a pilot hole with a smaller-diameter K-wire can further ensure smooth and precise impaction.

Regarding the intrinsic properties of the implants, K-wires lack threads and are therefore not susceptible to stability variations with respect to the direction of rotation, in contrast to screws, for which thread direction has been reported to affect stability.²⁶ This suggests that the DJ technique may offer uniform resistance against multidirectional rotational forces. The J shape inherently prevents pin migration, a known complication,^{13,27} and reduces the loss of initial fixation if minor placement errors occur compared to screws.

The hip joint angle for biomechanical testing was set at 114° flexion-extension and 6° abduction. This posture was chosen to approximate the mid-to-late stance phase of the feline gait cycle based on reports that the hip extends throughout stance and reaches maximum extension near the end of stance¹⁸ and kinematic analysis showing an extension extremum around 50% to 55% of the gait cycle.¹⁷ The 114° angle is an intermediate value between mean stance angles (approx equal to 102° to 104°) and maximum extension (approx equal to 130°), reflecting physiological posture while aligning the load axis nearly perpendicular to the SI joint. The 6° abduction angle also falls within the physiological range (neutral to

slight abduction) when considering coordinate-system differences between studies.^{17,18} Collectively, these parameters allowed the model to reproduce a natural weight-bearing orientation while minimizing torsional and shear components of the applied compressive load.

Sacroiliac luxation is a common pelvic injury in cats,¹ often requiring surgical stabilization.^{4,28} The DJ technique, which demonstrated superior mechanical performance, involves a unique in situ bending procedure. This technique might offer the advantage of requiring only a single lateral approach.²⁹ However, accurately creating the J shape and impacting the short portion may require considerable surgical skill as precise implant placement is crucial.³⁰ Recent advancements using fluoroscopy³¹ or computer navigation³ could enhance accuracy. Future studies exploring the feasibility of the DJ technique with minimally invasive approaches³² or 3-D-printed surgical guides are warranted. Long-term clinical outcomes and complication rates for the DJ technique are currently unknown.

This study has several limitations. First, the use of 3-D-printed PC models introduces differences from the in vivo environment. The material properties differ from bone, and the inability to replicate cancellous bone architecture may have influenced the assessment of screw purchase (group 1). As noted in similar studies,¹⁴ the absence of soft tissues underestimates in vivo stability. While the DJ group primarily failed due to K-wire bending, failure in native bone might involve microfractures due to lower compressive strength. However, using standardized PC models was essential to minimize confounding variables, such as varying bone quality, allowing for a focused comparison of the intrinsic mechanical performance of each fixation technique. Second, only a uniaxial static loading protocol was used, which does not capture the effects of cyclic loading or complex multidirectional forces relevant to fatigue resistance. Third, species differences must be considered when interpreting results alongside canine studies.^{10,12} Finally, while the 10° rotational failure criterion was based on previous literature,¹⁰ this threshold was derived through geometric conversion from a vertical displacement end point and has not yet been clinically validated in cats; therefore, its direct correspondence to true in vivo failure remains uncertain.

In this 3-D-printed feline SI luxation model, a newly devised DJ technique provided significantly greater rotational stiffness, maximum load resistance, and energy absorption than both SP and DK. These findings support the DJ technique as a biomechanically superior option for resisting rotational displacement in feline SI stabilization.

Acknowledgments

None reported.

Disclosures

The authors have nothing to disclose. No AI-assisted technologies were used in the composition of this manuscript.

Funding

The authors have nothing to disclose.


ORCID

Sang-Kun Jang  <https://orcid.org/0009-0002-7128-5886>


Yookyeong Lee  <https://orcid.org/0000-0003-1277-0590>


Sangyul Lee  <https://orcid.org/0009-0006-5984-4381>

Jaewon Do  <https://orcid.org/0009-0009-1173-0213>

Jeong-Woon Kim  <https://orcid.org/0009-0005-7736-7956>

Jun-Sik Cho  <https://orcid.org/0009-0002-4145-7384>

Hwi-yool Kim  <https://orcid.org/0000-0001-6237-9958>

Jung-Moon Kim  <https://orcid.org/0000-0002-6425-7716>

References

1. Bookbinder PF, Flanders JA. Characteristics of pelvic fracture in the cat. *Vet Comp Orthop Traumatol*. 1992;5(3):122-127. doi:10.1055/s-0038-1633081
2. Pratesi A, Grierson J, Moores A. Single transsacral screw and nut stabilization of bilateral sacroiliac luxation in 20 cats. *Vet Comp Orthop Traumatol*. 2018;31(1):44-52. doi:10.3415/VCOT-17-03-0047
3. Kleiner L, Wolf N, Precht C, Haenssngen K, Forterre F, Düver P. Feline sacroiliac luxation: comparison of fluoroscopy-controlled freehand vs. computer-navigated drilling in the sacrum—a cadaveric study. *Front Vet Sci*. 2025;11:1510253. doi:10.3389/fvets.2024.1510253
4. Bird FG, De Vicente F. Conservative management of sacroiliac luxation fracture in cats: medium- to long-term functional outcome. *J Feline Med Surg*. 2020;22(6):575-581. doi:10.1177/1098612X19867516
5. DeCamp CE. Fractures of the pelvis. In: Johnston SA, Tobias KM, eds. *Veterinary Surgery: Small Animal*. 2nd ed. Elsevier; 2017:938-956.
6. Fauron AH, Déjardin LM. Sacroiliac luxation in small animals: treatment options. *Companion Anim*. 2018;23(6):322-332. doi:10.12968/coan.2018.23.6.322
7. Bowlt KL, Shales CJ. Canine sacroiliac luxation: anatomic study of the craniocaudal articular surface angulation of the sacrum to define a safe corridor in the dorsal plane for placement of screws used for fixation in lag fashion. *Vet Surg*. 2011;40(1):22-26. doi:10.1111/j.1532-950X.2010.00761.x
8. Burger M, Forterre F, Brunberg L. Surgical anatomy of the feline sacroiliac joint for lag screw fixation of sacroiliac fracture-luxation. *Vet Comp Orthop Traumatol*. 2004;17(3):146-151. doi:10.1055/s-0038-1632803
9. Shales CJ, White L, Langley-Hobbs SJ. Sacroiliac luxation in the cat: defining a safe corridor in the dorsoventral plane for screw insertion in lag fashion. *Vet Surg*. 2009;38(3):343-348. doi:10.1111/j.1532-950X.2009.00509.x
10. Hanlon J, Hudson CC, Litsky AS, Jones SC. Mechanical evaluation of canine sacroiliac joint stabilization using two short screws. *Vet Surg*. 2022;51(7):1061-1069. doi:10.1111/vsu.13857
11. Radasch RM, Merkley DF, Hoefle WD, Peterson J. Static strength evaluation of sacroiliac fracture-separation repairs. *Vet Surg*. 1990;19(2):155-161. doi:10.1111/j.1532-950X.1990.tb01158.x
12. Kang A, Lee H, Lee A, Roh Y, Sim B, Jeong J. Biomechanical comparison of double 2.3-mm headless cannulated self-compression screws and single 3.5-mm cortical screw in lag fashion in a canine sacroiliac luxation model: a small dog cadaveric study. *Vet Comp Orthop Traumatol*. 2024;37(1):13-22. doi:10.1055/s-0043-1771508
13. Yap FW, Dunn AL, Farrell M, Calvo I. Trans-iliac pin/bolt/screw internal fixation for sacroiliac luxation or separation in cats: six cases. *J Feline Med Surg*. 2014;16(4):354-362. doi:10.1177/1098612X13503650
14. Jaroensong T, Lertjarugate K, Kumnuansil N, et al. Biomechanical assessment and comparison of fixation methods for bilateral sacroiliac joint luxation in 3D-printed

- feline pelvic bone models. *Vet World*. 2024;17(8):1798-1802. doi:10.14202/vetworld.2024.1798-1802
15. Nowotny J, Bischoff F, Ahlfeld T, et al. Biomechanical comparison of bi- and tricortical k-wire fixation in tension band wiring osteosynthesis. *Eur J Med Res*. 2019;24(1):33. doi:10.1186/s40001-019-0392-7
 16. Fedorov A, Beichel R, Kalpathy-Cramer J, et al. 3D Slicer. Version 1.0. Accessed June 21, 2024. <http://www.slicer.org>
 17. Guillot M, Gravel P, Gauthier ML, et al. Coxofemoral joint kinematics using video fluoroscopic images of treadmill-walking cats: development of a technique to assess osteoarthritis-associated disability. *J Feline Med Surg*. 2015;17(2):134-143. doi:10.1177/1098612X14537261
 18. Brown NP, Bertocci GE, Cheffer KA, Howland DR. A three dimensional multiplane kinematic model for bilateral hind limb gait analysis in cats. *PLoS One*. 2018;13(8):e0197837. doi:10.1371/journal.pone.0197837
 19. Choi Y, Cho JS, Choo Y, Kim S, Kim HY. Fully threaded headless cannulated screws provide similar biomechanical strength to conventional fixation in 3-dimensionally printed canine medial malleolar fracture models. *Am J Vet Res*. 2025;86(10):ajvr.25.03.0104. doi:10.2460/ajvr.25.03.0104
 20. Song Y, Wang M, Steven Baker J, Gu Y. The loading characteristics of landing in cats with different body weights. *Vet Med*. 2019;64(11):497-504. doi:10.17221/13/2019-VETMED
 21. Schnabl E, Bockstahler B. Systematic review of ground reaction force measurements in cats. *Vet J*. 2015;206(1):83-90. doi:10.1016/j.tvjl.2015.05.017
 22. Beer FP, Johnston ER, DeWolf JT, Mazurek DF. *Mechanics of Materials*. 7th ed. McGraw-Hill Education; 2014.
 23. Perren SM. Evolution of the internal fixation of long bone fractures. The scientific basis of biological internal fixation: choosing a new balance between stability and biology. *J Bone Joint Surg Br*. 2002;84(8):1093-1110. doi:10.1302/0301-620x.84b8.13752
 24. Philp H, Durand A, De Vicente F. Use of computed tomography to define a sacral safe corridor for placement of 2.7 mm cortical screws in feline sacroiliac luxation. *J Feline Med Surg*. 2018;20(6):487-493. doi:10.1177/1098612X17716847
 25. Garcia-Pertierra S, Meeson R, Yeung B, Bedford G, Pead M. Defining a safe corridor for trans-iliac pin placement in cats. *Aust Vet J*. 2021;99(6):242-248. doi:10.1111/avj.13062
 26. Bae S, Jeon Y, Lee H, Jeong J. Effect of thread direction on rotational stability in lag-screw fixation of sacroiliac luxation: an ex vivo cadaveric study in small-breed dogs. *Vet Surg*. 2025;54(2):311-320. doi:10.1111/vsu.14188
 27. Parslow A, Simpson DJ. Bilateral sacroiliac luxation fixation using a single transiliosacral pin: surgical technique and clinical outcomes in eight cats. *J of Small Anim Pract*. 2017;58(6):330-336. doi:10.1111/jsap.12659
 28. Decamp CE, Braden TD. Sacroiliac fracture-separation in the dog: a study of 92 cases. *Vet Surg*. 1985;14(2):127-130. doi:10.1111/j.1532-950X.1985.tb00841.x
 29. Singh H, Kowaleski M, McCarthy R, Boudrieau R. A comparative study of the dorsolateral and ventrolateral approaches for repair of canine sacroiliac luxation. *Vet Comp Orthop Traumatol*. 2016;29(1):53-60. doi:10.3415/VCOT-15-03-0051
 30. Déjardin L, Marturello D, Guiot L, Guillou R, DeCamp C. Comparison of open reduction versus minimally invasive surgical approaches on screw position in canine sacroiliac lag-screw fixation. *Vet Comp Orthop Traumatol*. 2016;29(4):290-297. doi:10.3415/VCOT-16-02-0030
 31. Jourdain M, Fernandes D, Védrine B, Gauthier O. Fluoroscopically-assisted closed reduction and percutaneous fixation of sacroiliac luxations in cats using 2.4 mm headless cannulated compression screws: description, evaluation and clinical outcome. *Vet Surg*. 2024;53(4):603-612. doi:10.1111/vsu.14070
 32. Tomlinson J. Minimally invasive repair of sacroiliac luxation in small animals. *Vet Clin North Am Small Anim Pract*. 2012;42(5):1069-1077. doi:10.1016/j.cvsm.2012.06.005